



Hadronic Final State Reconstruction in ATLAS at the LHC

Peter Loch
University of Arizona



This Talk

- 🌵 Introduction (Jet Finder Guidelines...)
- 🌵 Jet Calibration and Reconstruction
- 🌵 Missing E_T Reconstruction
- 🌵 Measurement Challenge: Pile-up from Minimum Bias Events;
- 🌵 "SLAC Jet/MET Retreat Tuples";
- 🌵 Conclusions;

"Disclaimers"

- most if not all plots shown are (naturally) based on simulations and have to be viewed within the corresponding limitations;
- most material shown here represents a snapshot of actual work in the relevant ATLAS groups and can in no way be understood as physics results - at most it indicates expectations;
- as a consequence, the material discussed here is very preliminary;

Physics Requirements for Jet and Missing E_T Measurements

- hadronic final state reconstruction requirements are stringent and often exceed what has been achieved in running experiments at Tevatron and HERA, for example;
- top reconstruction in $t\bar{t}$ events requires jet energy scale error of <1% absolute (immensely challenging!);
- jets need to be tagged to highest possible rapidities (~ 5) to enhance Higgs signal-to-background ratio in WW scattering production (order 10% of all Higgs over expected mass range);
- good missing E_T resolution also requires largest possible rapidity coverage;
- SUSY final state reconstruction also requires excellent hadronic calibration at a level of 1%;

Interesting:

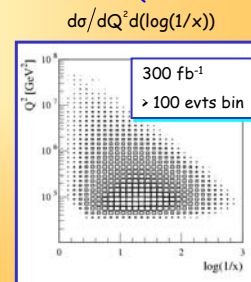
- increasing particle detection from $|\eta| < 3$ to $|\eta| < 5$ improves mass resolution for a light MSSM Higgs ($M_A = 150$ GeV) from 8 to 2 GeV;
- yet, quality requirements to forward particle measurements are relaxed \rightarrow most missing E_T is produced in the central region!

Required Energy Resolution

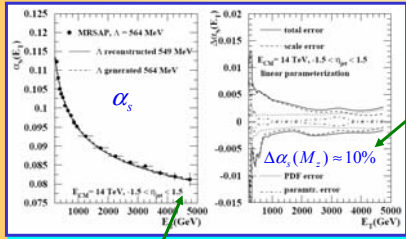
$$\sigma/E = \begin{cases} 50\%/\sqrt{E(\text{GeV})} \oplus 3\% & \text{for } |\eta| < 3 \\ 100\%/\sqrt{E(\text{GeV})} \oplus 6\% & \text{for } |\eta| > 3 \end{cases}$$

ATLAS requirements for hadronic (jet) energy resolution
 ATLAS Detector & Physics TDR CERN/LHCC/99-14/15

- hadronic (or jet) energy resolution is an important ingredient to the measurement error at LHC, even though we are very quickly dominated by systematics due to high event rate;
- nevertheless, one of the first distributions we have to understand are the QCD backgrounds to discovery physics channels and the parton distribution functions (PDFs) in yet uncovered kinematics regimes \rightarrow inclusive jet cross-section measurement (next slide);
- best illumination of kinematic region for PDF constraints, measuring the strong coupling at high mass scales, and detecting compositeness (probably more long term measurements) require good jet energy resolution as well;

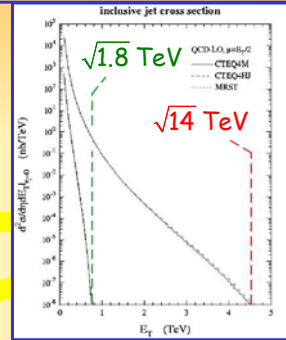


From the Inclusive Jet Cross-Section: Strong Coupling

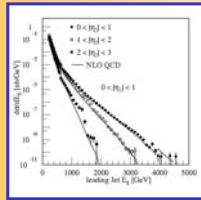


test of QCD at very small scale ($\alpha_s \approx 0.08$)

just from cross-section, can be improved by 3/2 jet ratio, but no competition for LEP/HERA!

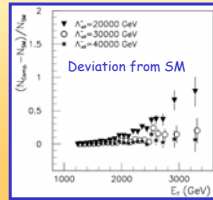


PDFs



di-jet cross section and properties (E_T, η_1, η_2) constrain parton distribution function

Compositeness



sensitivity to compositeness scale Λ up to 40 TeV @ 300 fb⁻¹ (all quarks are composites)

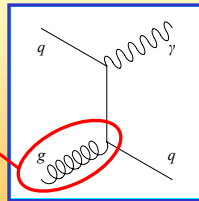
Other Jet Features at LHC:

statistical errors are small \rightarrow systematic uncertainties from jet algorithm, jet energy scale (mostly linearity of calorimeter response), and control of contributions from underlying event and pile-up dominate the total hadronic energy scale error rather quickly!

several calibration channels for jets ($W \rightarrow jj$, $Z/\gamma + \text{jet}(s)$) available with high statistics \rightarrow $\sim 1\%$ systematic error on energy scale possible;

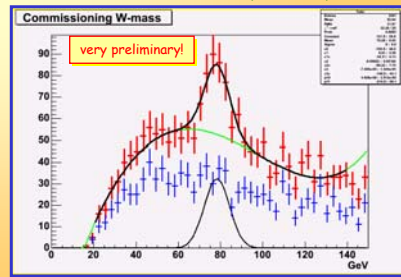
calibration measurements can be done in initial low luminosity running to minimize effects from pile-up events;

Dominant direct photon production gives access to gluon structure at high x ($\sim 0.0001-0.2$)



Process	σ (nb)	Evts/year ($\Lambda=10 \text{ fb}^{-1}$)
$W \rightarrow e\nu$	15	$\sim 10^8$
$Z \rightarrow e^+e^-$	1.5	$\sim 10^7$
$t\bar{t}$	0.8	$\sim 10^7$
Inclusive Jet Production	$p_T > 200 \text{ GeV}$	100 $\sim 10^9$
	$p_T > 1 \text{ TeV}$	0.1 $\sim 10^6$
	$p_T > 2 \text{ TeV}$	$10^{-4} \sim 10^3$
	$p_T > 3 \text{ TeV}$	$1.3 \times 10^{-6} \sim 10$

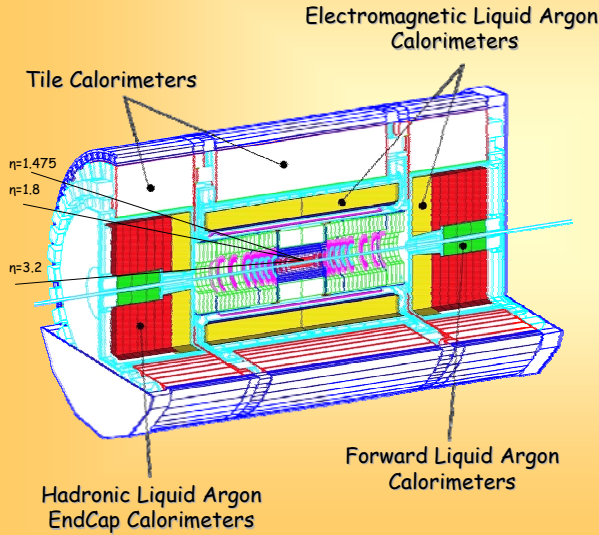
30 pb⁻¹ ~ 4 days @ 10^{33}



D. Pallin, ATLAS Calorimeter Calibration Workshop, Slovakia, Dec. 2004



The ATLAS Calorimeters



Electromagnetic Calorimeters:

- * Liquid Argon/Pb accordion structure;
- * highly granular readout (~170,000 channels);
- * $0.0025 \leq \Delta\eta \leq 0.05$, $0.025 \leq \Delta\phi \leq 0.1$;
- * 2-3 longitudinal samplings;
- * ~24-26 X_0 deep
- * covers $|\eta| < 3.2$, presampler up to $|\eta| < 1.8$;

Central Hadronic Calorimeters

- * Scintillator/Fe in tiled readout;
- * $\Delta\eta \times \Delta\phi = 0.1 \times 0.1$
- * 3 longitudinal samplings,
- * covers $|\eta| < 1.7$;

EndCap Hadronic Calorimeters

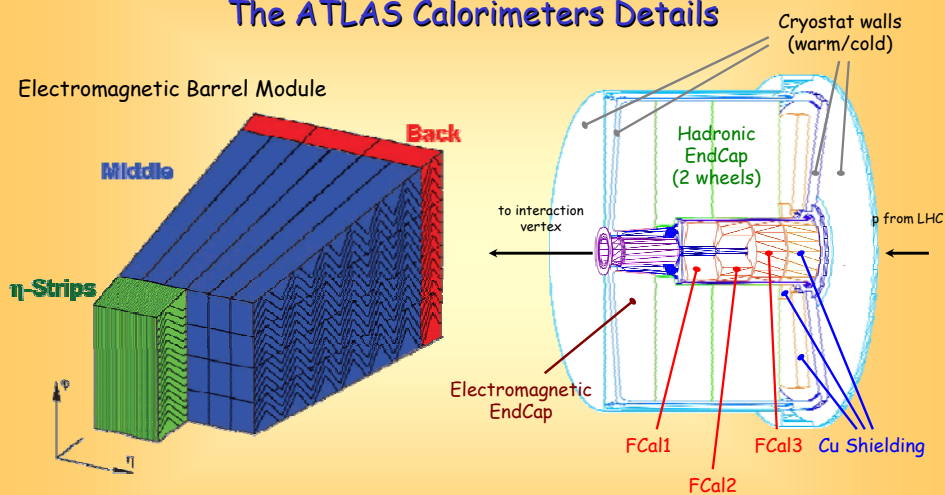
- * Liquid Argon/Cu parallel plate absorber structure;
- * $\Delta\eta \times \Delta\phi = 0.1 \times 0.1$ ($1.5 < |\eta| < 2.5$),
 $\Delta\eta \times \Delta\phi = 0.2 \times 0.2$ ($2.5 < |\eta| < 3.2$);
- * 4 samplings;

Forward Calorimeters

- * Liquid Argon/Cu or W absorbers with tubular electrodes in non-projective geometry;
- * $\Delta\eta \times \Delta\phi \approx 0.2 \times 0.2$ ($3.2 < |\eta| < 4.9$)
- * 3 samplings;



The ATLAS Calorimeters Details



total ~200,000 channels, with hadronic coverage ~10 absorption lengths in full acceptance ($|\eta| < 5$) and a typical level of non-compensation $e/h \approx 1.3-1.6$;



Jet Reconstruction Guidelines in ATLAS

Jets define the hadronic final state of any physics channel → jet reconstruction and calibration essential for signal and background definition;

But which jet algorithm to use ?
 Recommendations based on CDF & DØ experience from Tevatron Run I[†] very helpful;

Some "theoretical" requirements:

- infrared safety
- collinear safety
- invariance under boost
- order independence (same jet from partons, particles, detectors)

Some "experimental" requirements:

- detector (technology) independence
- minimal contribution to spatial and energy signal resolution (beyond effects intrinsic to the detector)
- stability with luminosity (!!, control of underlying event and pile-up effects)
- "easy" to calibrate, small algorithm bias to signal
- identify all physically interesting jets from energetic partons in pQCD (high reco efficiency!)
- efficient use of computing resources
- fully specified (pre-clustering, energy/direction definition, splitting and merging)

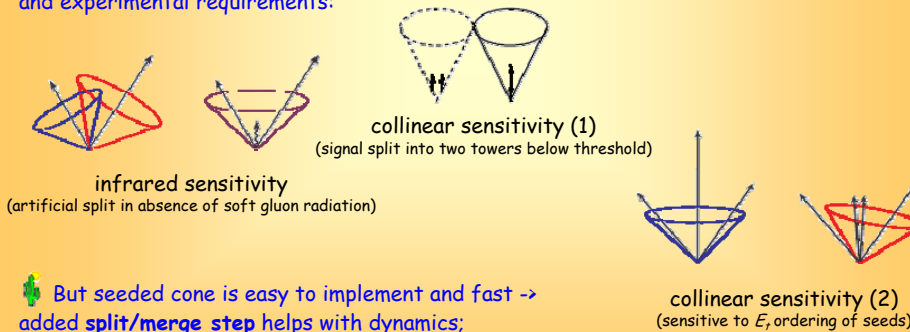
[†]G. Blazey et al., "Run II Jet Physics", hep-ex/0005012v2, 2000



Jet Finding Algorithm Implementations in ATLAS (1)

from guidelines + easy implementation → implemented K_T clustering (exploits kinematical correlations between particles) and (seeded and seedless) cone algorithm (geometrically motivated);

Seeded cone algorithm (most common and fast) has problems with some theoretical and experimental requirements:



But seeded cone is easy to implement and fast → added **split/merge step** helps with dynamics;

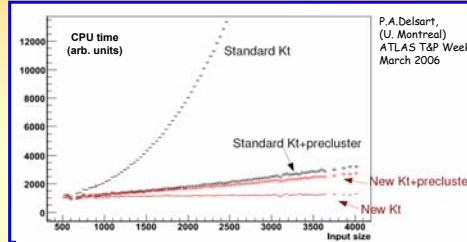
alternatively use K_T , **seedless cone** (typically slow, though!) and **mid-point cone**;

schematics from G. Blazey et al., "Run II Jet Physics", hep-ex/0005012v2, 2000



Jet Finding Algorithm Implementations in ATLAS (2)

K_t clustering avoids problems of cone finders, but can be very slow in standard implementation (CPU time $\sim n^3$) \rightarrow use pre-clustering to reduce number of kinematic objects on input or new **FastK_t** implementation; M.Cacciari/G.P.Salam hep-ph/0512210;



Common implementation details for all algorithms: **default 4-momentum recombination** in jet clustering procedures, user-defined pre- and final selections, signal treatment/pre-processing (e.g. calorimeter signals, see later), universal jet finder implementations,...

software design (jet event data model, jet algorithm implementations) provides universal jet finders (order independent?); can take **tracks**, **calorimeter cells**, **-towers**, **-clusters**, **energy flow objects**, and **MC truth objects** on input without code changes or adaptations;

new algorithms under consideration: "**Aachen**"-style **angular distance algorithm** - originally from M.Wobisch, ATLAS implementation by P.-A. Delsart (Montreal) **Optimal Jet Finder** - implementation by D.Lelas et al. (Victoria); and (soon) **two-pass mid-point**, initiated by J.Huston (Michigan), implementation by S. Thompson et al. (Glasgow);



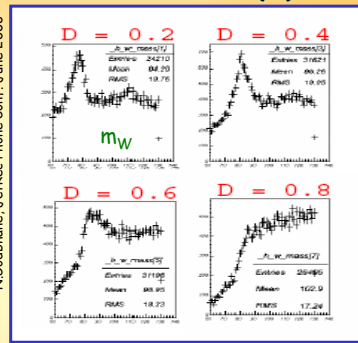
Jet Finding Algorithm Implementations in ATLAS (3)

jet algorithm parameters not universal - narrow jets generally preferred in busy events (**SUSY**, **ttbar** with **W \rightarrow jj**,...) to increase resolution power of final state; wider jets used in QCD for jet cross-section measurements to assure most complete/correct reconstruction of parton kinematics;

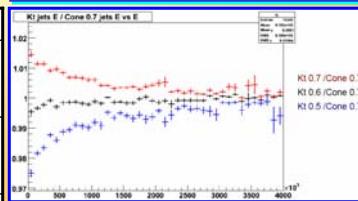
Standard jet collections provided for each event as in indicated in table below;

Discussions with CMS and theory suggested one common algorithm, likely 2-stage mid-point (c.f. J.Huston);

N.Godhame, JetRec Phone Conf. June 2006



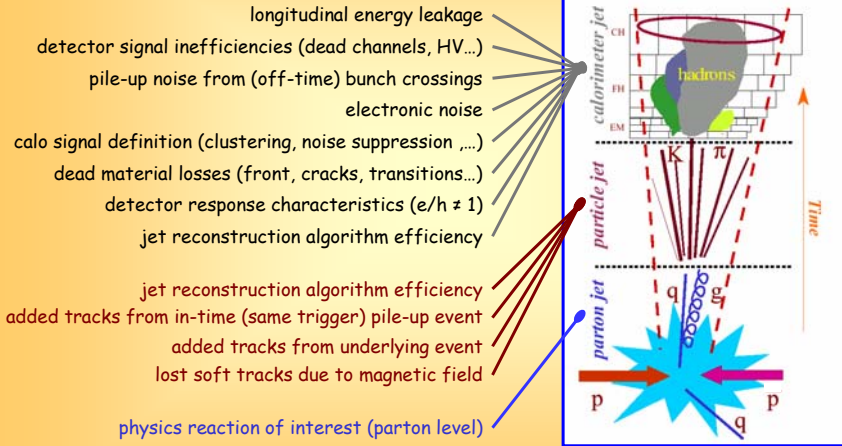
Algorithm	Cone Size R	Distance D	Clients
Seeded Cone	0.4		W mass spectroscopy, top physics
K _t		0.4	
Seeded Cone	0.7		QCD, jet cross-sections
K _t		0.6	
K _t		1.0	legacy



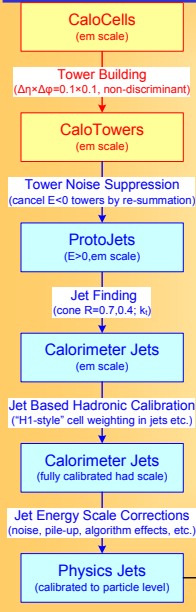
P.-A. Delsart, JetRec Phone Conf. June 28, 2006



Jet Reconstruction in the ATLAS Calorimeters



Calorimeter Jets Using Towers



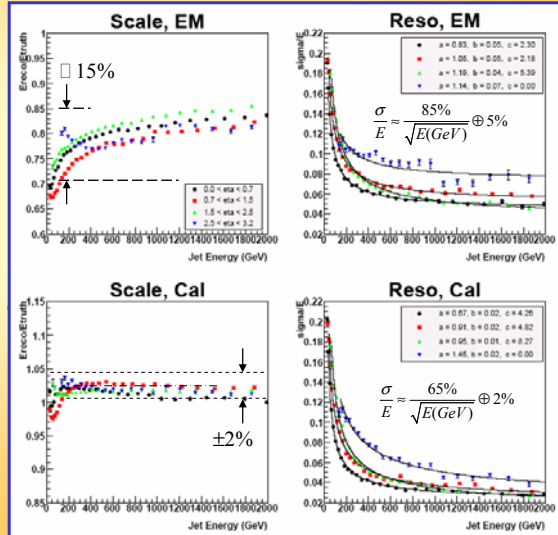
- all electromagnetic energy scale calorimeter cell signals are collected into projective towers (ideal detector geometry);
- noise cancellation by re-summation is applied to these towers, meaning towers with $E < 0$ are added to near-by towers with $E > 0$ until the resulting protojet has $E > 0$ (all cells are kept!);
- jet finding is run on the protojets, resulting in "uncalibrated" electromagnetic energy scale calorimeter tower jets;
- the cells in a jet are retrieved using object navigation, and cell signal weights are applied based on cell energy density and location (default) to compensate and correct signals for $e/h \neq 1$ and inactive material losses \rightarrow hadronic energy scale jets;
- additional corrections for residual E , and η dependencies are applied \rightarrow jets are calibrated to particle level (see next slide);
- additional corrections possibly derived from $W \rightarrow jj$, photon/Z+jet(s) could be applied \rightarrow careful, potential biases due to collision physics environment! \rightarrow no default today for good reasons! \rightarrow no general refined physics jet yet!



ATLAS Jet Calibration

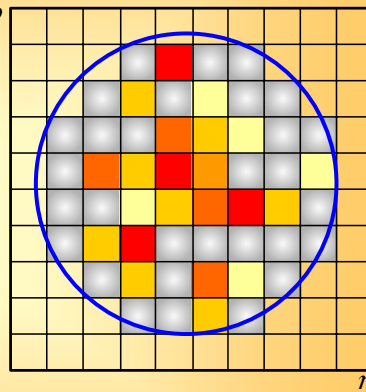
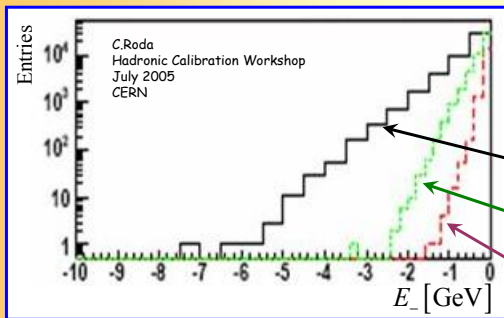
Chiara Roda HCP 2006

- several schemes under study, most developed (default) scenario is based on fitting cell signal weights based on signal densities in cone jets (R=0.7) in fully simulated QCD di-jet events → motivated by H1 signal weighting technique;
- also apply (Et,η) dependent overall jet energy corrections to adapt for other jet algorithms (new feature since 12.0.4);
- clearly only possible in MC → fitting of weights requires choosing truth reference (particle level jets found with the same algorithm, particles pointing into direction of calorimeter jet...);



Problems with Towerjets

- use of (quasi-projective) calorimeter cell towers as input to jet finding includes too many non-signal cells into jets due to longitudinal summation and fixed area coverage (non-discriminating summation of cells in tower);
- additional sources of noise → attempt to cancel noise by tower re-summation (add "negative" towers to nearby ones with positive signals);



$$E_- = \sum_{E_c < 0} E_c \text{ (in CaloTowerJets)}$$

$$E_- = \sum_{E_c < 2\sigma_{noise}} E_c \text{ (in CaloTowerJets)}$$

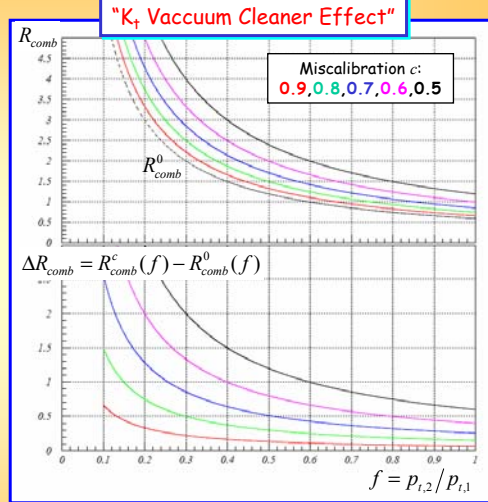
$$E_- = \sum_{E_c < 0} E_c \text{ (in CaloTopoClusterJets)}$$



Problems with "Uncalibrated Input"

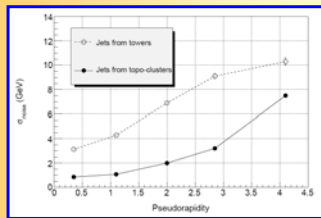
- 🌵 tower signals used in jet finding calibrated on electromagnetic energy scale -> relative calibration of jet input can be 30% (or more!) off if hadronic!
- 🌵 not too big a problem for cone jets (tbc), but affects shape of K_T jets;
- 🌵 in particular, K_T jets can get much wider if constituent signal too low;
- 🌵 relative uncalibrated input also problematic for kinematic cuts on this input!

Radius $R_{comb} = \sqrt{\Delta\eta^2 + \Delta\phi^2}$ up to which two objects are combined by the K_T algorithm, as function of the p_T ratio of the constituents, with $p_{T,1} > p_{T,2}$ (objects are always combined for $p_{T,1} < p_{T,2}$ if $R_{comb} < D$)



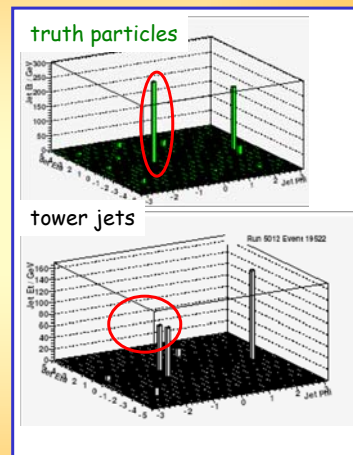
Tower Jet Issues

- 🌵 use of (quasi-projective) calorimeter cell towers as input to jet finding includes too many non-signal cells into jets due to longitudinal summation and fixed area coverage (non-discriminating summation of cells in tower) -> needs tower resummation for (coarse) noise suppression;



I.Vivarelli, Calorimeter Calibration Workshop, September 2006

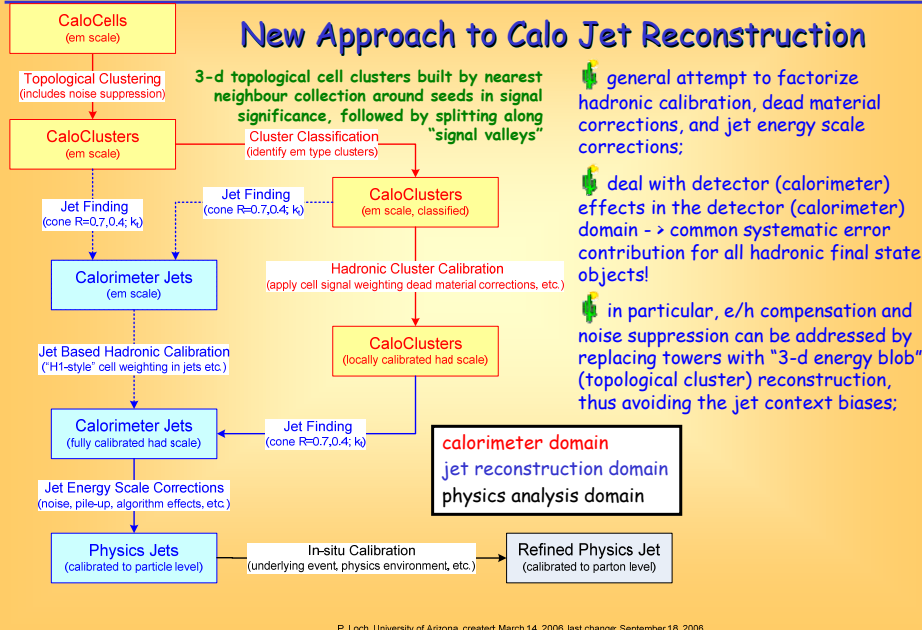
- 🌵 fixed tower grid potentially introduces artificially split seeds, which can be reduced by lowering the seed cut from 2 GeV to 1 GeV (now the default);



I.Vivarelli, Calorimeter Calibration Workshop, September 2006



New Approach to Calo Jet Reconstruction



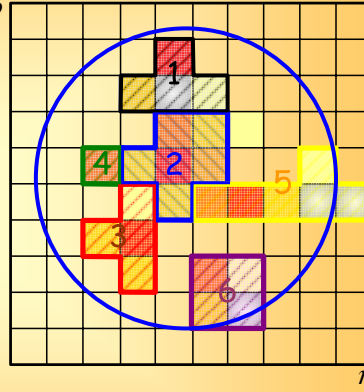
Jet Reconstruction from Clusters

- form topological cell clusters
 - efficient and least biased noise suppression ideally provides calorimeter signals of fixed significance with respect to the underlying electronic and pile-up noise;
- calibrate clusters to hadronic energy scale (not jet energy scale!)
 - topological clusters can be calibrated with this respect ("local calibration") using deposited energies and signals in (pion) MC at cell level;
 - calibration includes cluster classification, hadronic signal weighting, and dead material corrections;
 - this takes care of many detector effects (e/h, energy losses in upstream and internal dead material...);
 - already very useful as input to missing transverse energy calculations;
 - note that local cluster calibration derived from MC can be applied to testbeam pions for comparisons!!
- use calibrated clusters as input to jet finding
 - reduce potential 30% relative miscalibration to ~5% or so -> enhance jet reconstruction stability, especially for K_T ;
- apply jet energy scale corrections
 - very specific corrections dependent on jet algorithm and algorithm parameters, physics environment (underlying event contribution, final state multiplicities and particles,...);
 - one or two step normalization: directly to parton level derived from Z/γ +jet(s) or W ->jj (careful about biases!) or first particle level corrections, then particle->parton level corrections;

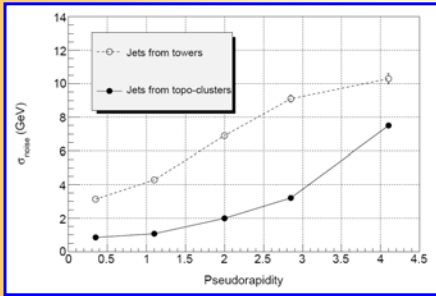
Calorimeter Hadronic Signal Definition

topological clustering in three dimensions, with φ local maxima based splitting, attempts to reconstruct cell signal correlations created by shower development;

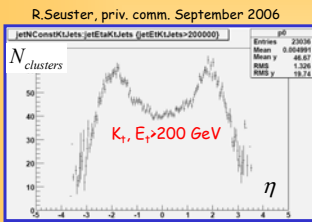
implements noise suppression based on signal significance of cell and (!!) its neighbours \rightarrow much less noise cells included in hadronic calorimeter signal, but some small signal bias unavoidable;



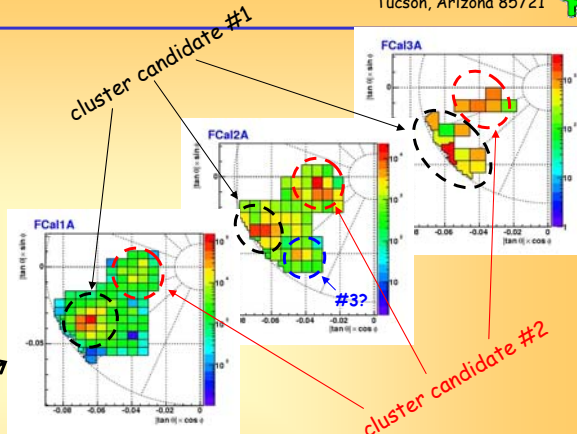
some sensitivity to shower structures allows classification/tagging of clusters \rightarrow selective and optimized calibration procedures for individual clusters possible;



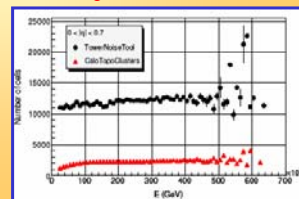
I.Vivarelli, Calorimeter Calibration Workshop, September 2006



drop in #clusters in central region reflects granularity of calorimeter (relative cell size wrt to shower sizes)



Topological Clusters in (Forward) Jets



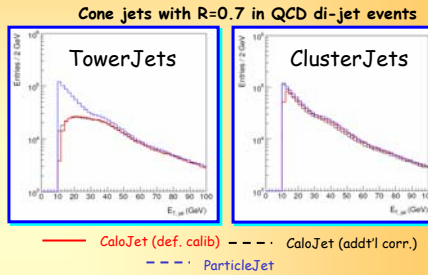
I.Vivarelli, CCW 2006, September 2006



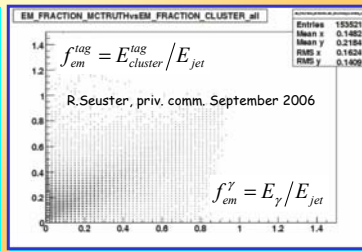
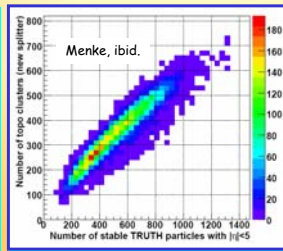
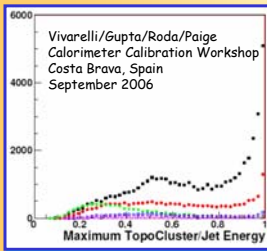
Early Observations for Jets from Topoclusters

jet finding efficiency for topoclusters: jet seeds seem to be more efficiently found due to the combination of cell signals and free location in the calorimeter (especially for low energetic jets); towers can actually reduce the jet finding efficiency due to their fixed grid event view with possible splitting seed energy deposit into signals below threshold (shower spread distorts "perfect" transverse energy flow in cone);

additional cluster features like em tagging can help with jet characterization and calibration;



F. Paige, private communications, May 2006

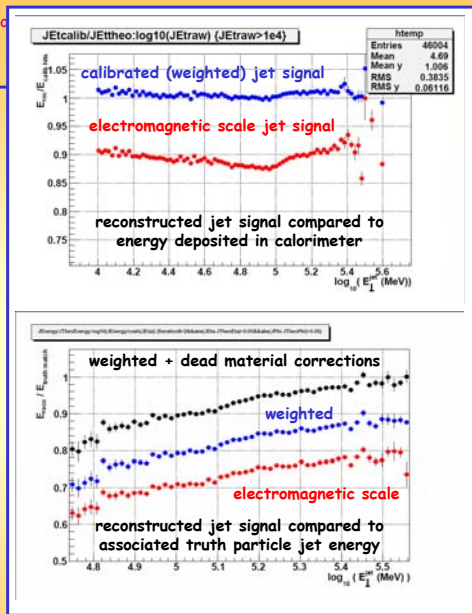


Cluster Jets Under Study

"local" cluster-based hadronic calibration compensates for e/h → can reconstruct energy deposited in sensitive calorimeter by pions or jets by using calibration functions derived from pions;

incoming particle and jet energy reconstruction requires additional corrections for dead material energy losses for hadronic and electromagnetic clusters, out-of-cluster signal losses (introduced by noise suppression strategy and resulting cluster formation strategies), scale corrections for electromagnetic clusters → all under intensive study for upcoming release 13.0.0;

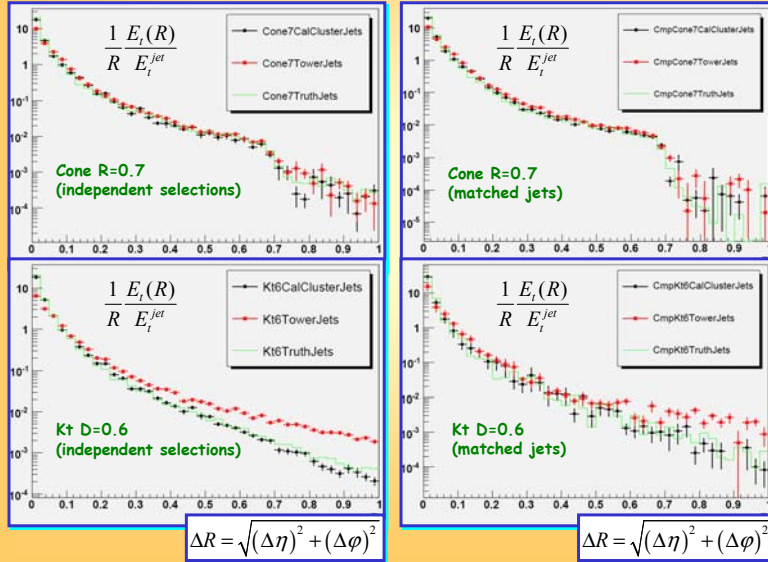
additional corrections needed in jet context for particle losses in magnetic field, disconnected energy deposits without any signal, jet algorithm algorithm biases, accidental contributions from underlying or (later) pile-up events...



Sven Menke, Calorimeter Performance Meeting, December 6, 2006



Differential Jet Shapes in Towers and Clusters

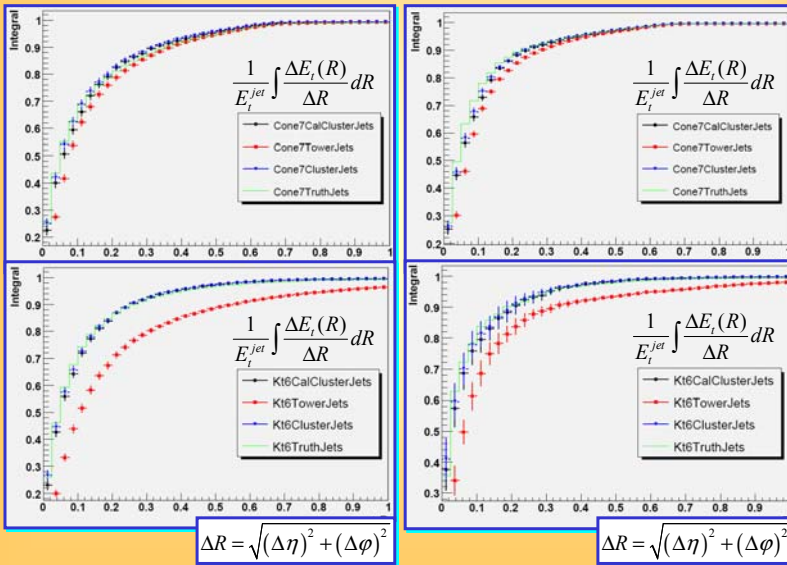


very, very preliminary!

Relative contribution of jet constituents to transverse jet energy, measured as function of the distance of the constituents to the jet axis and normalized to this distance



Integrated Jet Shapes in Towers and Clusters

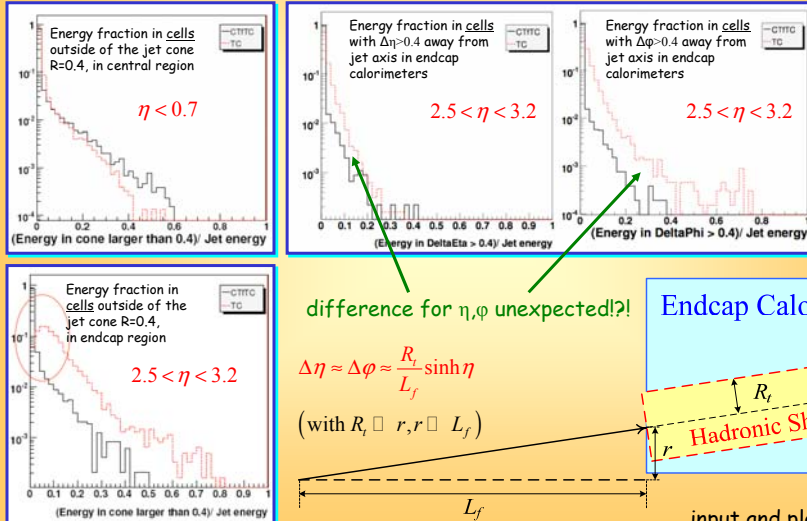


very, very preliminary!

Integrated relative contribution of jet constituents to transverse jet energy, measured as function of the distance of the constituents to the jet axis and normalized to this distance



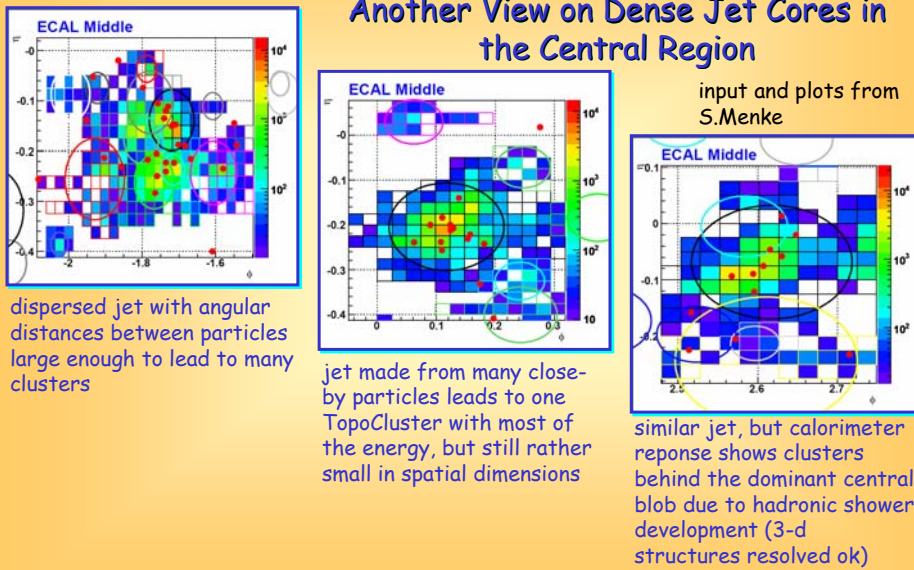
Problems (or Features) of ClusterJets



(red are $R=0.4$ cone jets from TopoClusters, black are jets from towers built from cells in TopoClusters, to take advantage of the noise suppression)



Another View on Dense Jet Cores in the Central Region

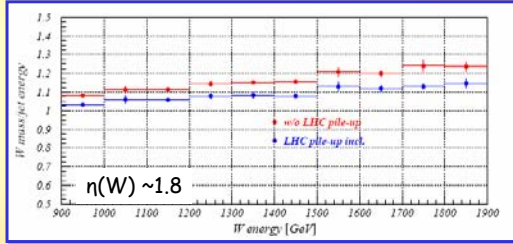




Final Jet Calibration

using fully calibrated and corrected clusters in jet finding reduces the problem of jet calibration to the understanding of the contributions from the jet algorithm inefficiencies, the underlying events, and the overall event topology possibly including pile-up;

$W \rightarrow jj$ can help to estimate these final corrections, but are mostly found in a very specific $\bar{t}\bar{t}$ topology (bias?), and with special jets (no color link to rest of event); also, there are kinematical limits on the effectiveness of this calibration signal - order(3%) more likely than 1% today;



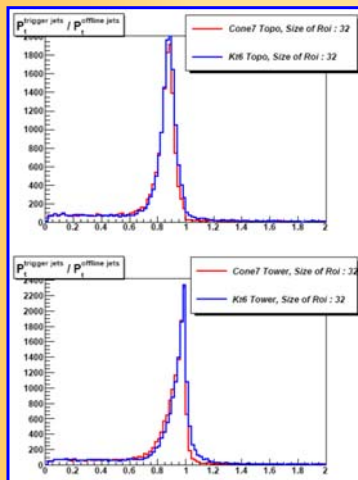
P. Savard, P. Loch, CALOR97

other channels like Z +jet(s) or photon+jet(s) can help, but good understanding of initial and final state radiation needed (modeling); also, kinematical limit for 1% is about 400 GeV or so;

very hard (~TeV) jet energy scale validation under study - likely with QCD di-jets and bootstrapping from kinematic regime of photon/ Z +jet(s); some worry about precision and bias;



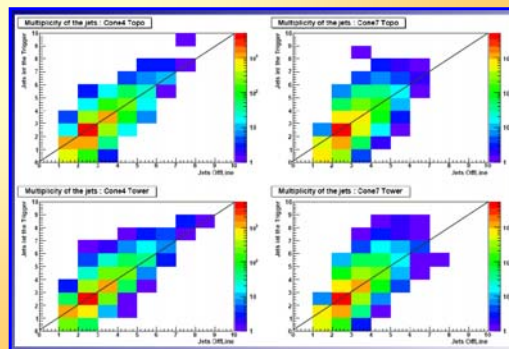
Jets HLT Studies



B. Brellier, P.-A. Delsart, ATLAS Canada Meeting August 21, 2006

cluster and tower jets reconstructed in ROI instead of full event, using same cuts and calibration as in offline jet reconstruction;

jet multiplicities and energies very comparable considering the limited ROI information;



B. Brellier, P.-A. Delsart, ATLAS Canada Meeting Aug. 21, 2006

Selected Other Ongoing and New Efforts

T. LeCompte, Feb. 20, 2007

- very first look at L1 turn-on curve (T. LeCompte): jets in SUSY with L1 threshold 56 GeV (approx. 70 GeV in precision reconstruction);

- preparation for first data/low lumi running: **in-situ jet calibration** determination and validation with photon/Z+jet(s) (Barcelona, Chicago, Heidelberg, TRIUMF,...), di-jet balance (Sheffield, Wisconsin, SLAC,...), low Pt single hadron tracks in minbias events (Melbourne);

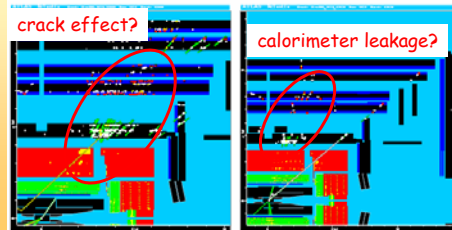
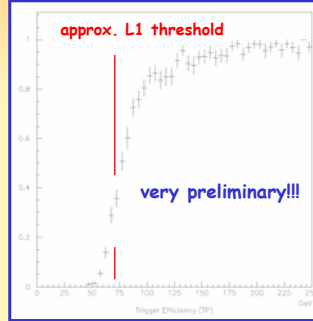
- energy scale validation for very hard jets (Glasgow, Heidelberg, Tokyo,...);

- forward jets in VBF and others (ITEP, Bonn,...);

- ATLFAST jet calibration (Pisa,...);

- use of tracks for jet calibration refinement (SLAC) and general characterization (Victoria);

.....



Frank Paige, Jet/EtMiss/τ performance meeting, ATLAS T&P Week February 2006

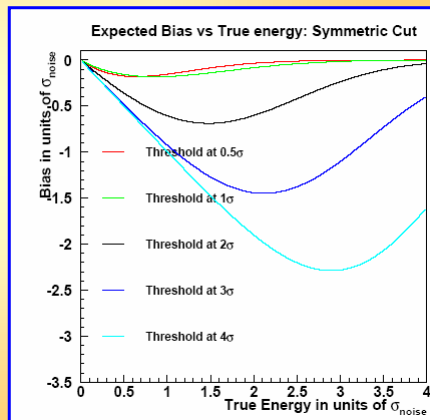
Missing Transverse Momentum Reconstruction

- best missing E_T calculation is using calibrated cell signals and all cells with true signal;

- in a real detector this calculation is very sensitive to electronic noise (at least) - typically 70-90% of all cells in ATLAS have no true or significant signals;

- symmetric or asymmetric cell noise cuts reduce the fluctuations significantly, but introduce a bias (shift off 0) due to this cut;

- topological clustering imposes a noise cut, but lets cells survive based in the signal in their neighbours → less bias, yet near optimal suppression of incoherent (electronics) noise;

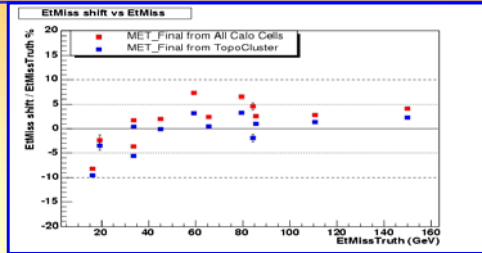


K. Cranmer, in talk by S. Menke, ATLAS Physics Workshop 07/2005

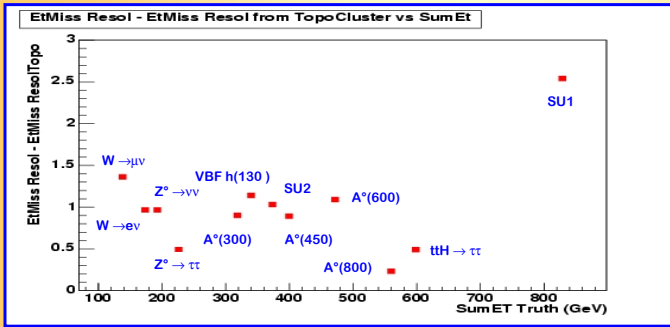


Missing Et Reconstruction

calculating missing E_T from topological clusters brings a small improvement in the bias;



S. Resconi, ATLAS Physics Workshop 07/2005



S. Resconi, ATLAS Physics Workshop 07/2005

calculating missing E_T from topological clusters improves the missing Et resolution for many physics channels;

$$\sigma_{ExMiss} \approx 47\% \cdot \sqrt{\sum E_{T,i}}$$



Default Missing Et Calculation

MET_RefFinal

=

MET_Calib

+

MET_Cryo

+

MET_Muon

Calorimeter Cells
 $|E_{cell}| > 2\sigma_{noise}$
 calibrated with weights from jet calibration
 "H1" style jet calibration

Cryostat Losses EMB/Tile
 correction factors from reconstructed seeded cone tower jets with $\Delta R = \Delta\eta \times \Delta\phi \leq 0.7$
 based on cone tower jets

MuonBoy
 $|\eta| \leq 2.7$
 best match/good quality required
 p_T from external spectrometer

Calorimeter Cells
 in TopoClusters ($4\sigma/2\sigma/0\sigma$)
 calibrated with weights from jet calibration
 "H1" style jet calibration

Cryostat Losses EMB/Tile
 correction factors from reconstructed seeded cone topocluster jets with $\Delta R = \Delta\eta \times \Delta\phi \leq 0.7$
 based on cone cluster jets

MOORE
 $|\eta| \leq 2.7$
 best match/good quality required
 p_T from external spectrometer

Calorimeter Cells
 in TopoClusters ($4\sigma/2\sigma/0\sigma$)
 cluster based calibration/dead material correction
 local hadronic calibration

Cryostat Losses EMB/Tile
 correction factors from reconstructed k_T topocluster jets with $D = 0.6$
 based on k_T cluster jets

Exclusively uses officially released calibrations from all sub-systems!

Calorimeter Cells
 in e^+ , γ , τ jets, unused TopoClusters, outside weights from physics object calibration
 refined calibration

each contribution is individually available in AOD/ESD \rightarrow some degree of freedom in physics analysis;

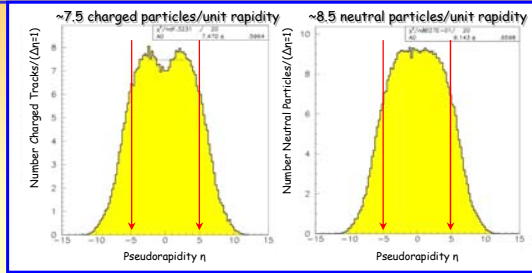
Calorimeter Cell Clusters
 TopoClusters ($4\sigma/2\sigma/0\sigma$)
 cluster based calibration/dead material correction
 local hadronic calibration

not possible to go back to finest detector granularity in AOD (e.g. calorimeter cells);

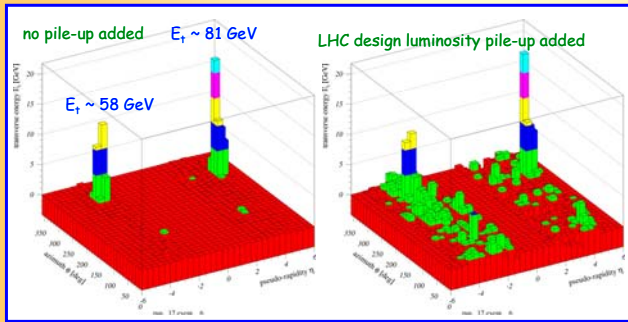
highlighted combination recommended even though still some improvements in refined calibration expected (incomplete);

Pile-Up

high lumi, large $\sigma_{\text{incl}} \approx 80 \text{ mb} \rightarrow \sim 23$ min bias events/bunch crossing, with ~ 75 charged tracks/event within typical detector acceptance $|\eta| < 5$ at $10^{34} \text{ cm}^{-2}\text{s}^{-1}$;



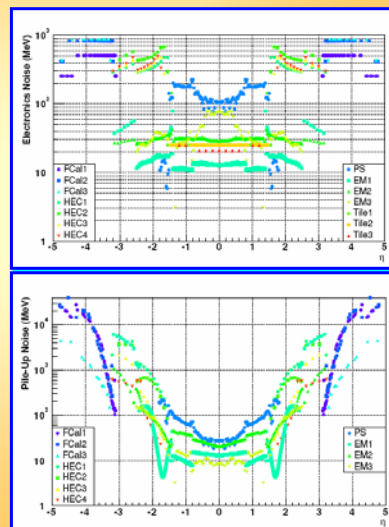
ATLAS Calorimeter Performance Technical Design Report CERN/LHCC 96-40



effect of pile-up depends on detector technology and readout electronics - long bi-polar shaping functions in ATLAS calorimeters lead to out-of-time contributions with negative signals;

Pile-Up vs Electronic Noise in Calorimeter Cells

- cell signal fluctuations introduced by pile-up dominate wrt electronics noise in the ATLAS endcap calorimeters, but are comparable to, or less than, electronic noise in the central calorimeters;
- pile-up fluctuations in a given cell are not Gaussian due to the lateral and longitudinal coupling of signals in neighbouring cells introduced by the showers in minimum bias events;
- still, pile-up RMS in each cell (a function of the instantaneous luminosity) can be used to define the significance of the cell signal to first order;
- still more detailed studies are needed to understand the structure (mini-jets, etc...) in the pile-up events, and to find a measure for the instantaneous lumi for each triggered event (correlation between forward energy flow and pile-up ?);

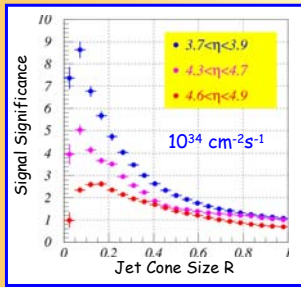


S. Menke, ATLAS Physics Workshop 07/2005



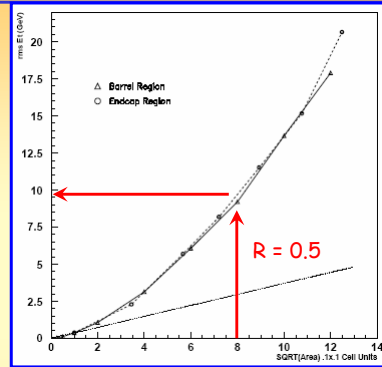
Pile-Up in Jets

- typically around 10 GeV E_T signal fluctuations in jet cone of $R = 0.5$ at design luminosity;
- this finding is rather independent of η ;



P. Loch & P. Savard, CAL0997

Forward tag jets in Higgs production have average E_T of 30-50 GeV only (decreasing with increasing η)



P. Savard et al., ATLAS-CAL-NO 084/1996

- forward jet detection is non-trivial (low significance of signal even in smallest jet cone);
- further studies needed to understand pile-up contributions to other jet finders;



This Retreat

- various physics simulations used to produce CNTAA from ESD
 - 12.0.3 + private tags (all in development branch for 13);
 - calorimeter: re-do all clusters and towers for hadronic final state
 - jet: re-do all calorimeter and truth jet finding;
 - typically (1...many) 1000's of events;
 - not quite official tuple!
- available physics (Ariel knows technical details on file locations, names,...):
 - QCD (J_x , $x=1, \dots, 8$);
 - W+jets, $W \rightarrow e + \text{neutrino}$;
 - top;
 - SUSY (SU2);
 - minimum bias
- jets
 - Seeded Cone $R=0.7$, Seeded Cone $R=0.4$; $K_t D=0.6$, $K_t D=0.4$;
 - towers (0.1x0.1), topological cell clusters (em scale), topological cell clusters (hadronic scale);
- missing ET
 - well documented in Wiki page <https://twiki.cern.ch/twiki/bin/view/Atlas/TauEtMiss>;
 - click on Etmis reconstruction and calibration;



Webpage under development (1)...

TUPLE VARIABLES: JET, CLUSTERS, AND MISSING E_T

Table of Content

1.Introduction and Disclaimers

2.Global Jet Variables

1.Introduction and Disclaimers

This page contains some documentation for the root-tuple variables available for the SLAC Jet/MissingEt retreat March 2007. The tuples have been produced from **csc11** production, which in large parts used Athena release 11.0.42 and some 11.0.5[†]. The content of the tuples is selective, with a focus on the calorimeter signal and jet algorithms. Generally, there are variables for vertices, tracks (**TrackParticle** objects), **egamma** object variables (*not* **Electron**), sliding window and topological cluster variables for electron reconstruction, uncalibrated and (first order) calibrated topological clusters for jets, missing E_T blocks from various sources, and muons from the **MuID** package.

The data structure is flat, i.e. all variables independent of their type are leaves of only one tree in **root**. The *Athena Aware Ntuple* (CBNTAA) technology has been used to book and fill the variables. The production code is based on release 12.0.3, with several new tags for jet reconstruction and CBNTAA jet code now available in the main development branch (toward 13.0.0). The main difference to 12.0.6 and the main branch may be a slightly different local hadronic calibration package lacking the recent improvements concerning dead material corrections, cluster tagging, and out-of-cluster corrections.

[†]11.0.5 includes trigger information which is *not included* in the tuples available for this retreat.

Attention!

Some of the variable names used for clusters and jets in this version of the root tuple are not (yet) standard. We expect most of them to become the standard for 13.0.0, though. Some may of course disappear, too!



Webpage under development (2)...

2.Global Jet Variables

The jet data available in the tuple reflects physics requirements and allows quite detailed performance studies for different jet algorithm and signal sources. To separate the various sources and algorithms, the following convention has been used²:

`jet{VarName}_{Algorithm}{Parameter}{SignalSource}`

The algorithm indicator **{Algorithm}** and the **{Parameter}** are summarized in the table to the right. The algorithms and their parameter space considered for the tuple corresponds to the standard jet collections available in default reconstruction.

The available signal sources (**{SignalSource}** parameter) are

Truth	jets from (stable) particles in the truth event in Monte Carlo;
Tower	jets from projective calorimeter cell towers (size $\Delta\eta \times \Delta\phi = 0.1 \times 0.1$);
CalClus	jets from calibrated topological clusters (hadronic energy scale, corrected for $e/h > 1$ and some dead material), reconstructed using 4/20 cell signal significance cuts (in σ_{noise} , as seed/neighbour/perimeter cell cut);
Clus	jets from uncalibrated topological clusters (electromagnetic energy scale, no further corrections), reconstructed using 4/20 cell signal significance cuts (in σ_{noise} , as seed/neighbour/perimeter cell cut);

The global jet variables available for all jets, independent of the signal source, are:

{Algorithm}	{Parameter}	Algorithm
C	4	Seeded Cone Algorithm with cone size $R = 0.4$
	7	Seeded Cone Algorithm with cone size $R = 0.7$
Kt	4	K_t Algorithm with distance parameter $D = 0.4$
	6	K_t Algorithm with distance parameter $D = 0.6$



More details for Jets

Seeded Cone R=0.7 Jet Finder					
Variable Name	Type	Truth	Tower	TopoCluster	Calibrated TopoCluster
njets	UInt_t	jetNum_C7Truth;	jetNum_C7Tower;	jetNum_C7Clus;	jetNum_C7CalClus;
pseudorapidity	vector<double>	jetEta_C7Truth;	jetEta_C7Tower;	jetEta_C7Clus;	jetEta_C7CalClus;
azimuth	vector<double>	jetPhi_C7Truth;	jetPhi_C7Tower;	jetPhi_C7Clus;	jetPhi_C7CalClus;
energy	vector<double>	jetE_C7Truth;	jetE_C7Tower;	jetE_C7Clus;	jetE_C7CalClus;
transverse energy	vector<double>	jetEt_C7Truth;	jetEt_C7Tower;	jetEt_C7Clus;	jetEt_C7CalClus;
mass	vector<double>	jetM_C7Truth;	jetM_C7Tower;	jetM_C7Clus;	jetM_C7CalClus;
Px	vector<double>	jetPx_C7Truth;	jetPx_C7Tower;	jetPx_C7Clus;	jetPx_C7CalClus;
Py	vector<double>	jetPy_C7Truth;	jetPy_C7Tower;	jetPy_C7Clus;	jetPy_C7CalClus;
Pz	vector<double>	jetPz_C7Truth;	jetPz_C7Tower;	jetPz_C7Clus;	jetPz_C7CalClus;
number of constituents	vector<long>	jetSize_C7Truth;	jetSize_C7Tower;	jetSize_C7Clus;	jetSize_C7CalClus;
electromagnetic energy fraction	vector<double>	jetEmf_C7Truth;	jetEmf_C7Tower;	jetEmf_C7Clus;	jetEmf_C7CalClus;
constituent final energy	vector<vector<double>>	jetCEf_C7Truth;	jetCEf_C7Tower;	jetCEf_C7Clus;	jetCEf_C7CalClus;
constituent final Px	vector<vector<double>>	jetCEPf_C7Truth;	jetCEPf_C7Tower;	jetCEPf_C7Clus;	jetCEPf_C7CalClus;
constituent final Py	vector<vector<double>>	jetCEPyf_C7Truth;	jetCEPyf_C7Tower;	jetCEPyf_C7Clus;	jetCEPyf_C7CalClus;
constituent final Pz	vector<vector<double>>	jetCEPzf_C7Truth;	jetCEPzf_C7Tower;	jetCEPzf_C7Clus;	jetCEPzf_C7CalClus;
constituent final pseudorapidity	vector<vector<double>>	jetCEEtaf_C7Truth;	jetCEEtaf_C7Tower;	jetCEEtaf_C7Clus;	jetCEEtaf_C7CalClus;
constituent final azimuth	vector<vector<double>>	jetCEPhif_C7Truth;	jetCEPhif_C7Tower;	jetCEPhif_C7Clus;	jetCEPhif_C7CalClus;
constituent final kinematic weight	vector<vector<double>>	jetCWF_C7Truth;	jetCWF_C7Tower;	jetCWF_C7Clus;	jetCWF_C7CalClus;
constituent reference	vector<vector<double>>	jetCRef_C7Truth;	jetCRef_C7Tower;	jetCRef_C7Clus;	jetCRef_C7CalClus;
constituent raw energy	vector<vector<double>>			C7ClusJetCluE;	C7CalClusJetCluE;
constituent cluster tag	vector<vector<double>>			C7ClusJetCluTag;	C7CalClusJetCluTag;
constituent cluster center X	vector<vector<double>>			C7ClusJetCluXi;	C7CalClusJetCluXi;
constituent cluster center Y	vector<vector<double>>			C7ClusJetCluYi;	C7CalClusJetCluYi;
constituent cluster center Z	vector<vector<double>>			C7ClusJetCluZi;	C7CalClusJetCluZi;
constituent electromagnetic fraction raw	vector<vector<double>>			C7ClusJetCluFemf;	C7CalClusJetCluFemf;
constituent electromagnetic fraction final	vector<vector<double>>			C7ClusJetCluFemf;	C7CalClusJetCluFemf;

Will be on the web!



More details for Clusters

Uncalibrated TopoClusters	Calibrated TopoClusters	Type	Comment	
cl_ectuster_rawtopo;	cl_ectuster_caltopo;	float_t	total cluster energy sum in event	CT
cl_nc_rawtopo;	cl_nc_caltopo;	int_t	number of topo-clusters in tuple	
cl_nctotal_rawtopo;	cl_nctotal_caltopo;	int_t	total number of topo-clusters	Cluster Kinematic
cl_e_rawtopo;	cl_e_caltopo;	vector<float>	cluster energy	
cl_et_rawtopo;	cl_et_caltopo;	vector<float>	transverse energy	Cluster Kinematic
cl_eta_rawtopo;	cl_eta_caltopo;	vector<float>	cluster pseudorapidity	
cl_phi_rawtopo;	cl_phi_caltopo;	vector<float>	cluster azimuth	Cluster Kinematic
cl_nofocells_rawtopo;	cl_nofocells_caltopo;	vector<long>	# cells in cluster	
cl_nscop_etf_rawtopo;	cl_nscop_etf_caltopo;	vector<long>	cluster reconstruction status	Cluster Kinematic
cl_eemb0_rawtopo;	cl_eemb0_caltopo;	vector<float>	energy in barrel pre-sampler	
cl_eemb1_rawtopo;	cl_eemb1_caltopo;	vector<float>	energy in barrel sampling 1	Cluster Kinematic
cl_eemb2_rawtopo;	cl_eemb2_caltopo;	vector<float>	energy in barrel sampling 2	
cl_eemb3_rawtopo;	cl_eemb3_caltopo;	vector<float>	energy in barrel sampling 3	Cluster Kinematic
cl_eeemb0_rawtopo;	cl_eeemb0_caltopo;	vector<float>	energy in endcap pre-sampler	
cl_eeemb1_rawtopo;	cl_eeemb1_caltopo;	vector<float>	energy in endcap sampling 1	Cluster Kinematic
cl_eeemb2_rawtopo;	cl_eeemb2_caltopo;	vector<float>	energy in endcap sampling 2	
cl_eeemb3_rawtopo;	cl_eeemb3_caltopo;	vector<float>	energy in endcap sampling 3	Cluster Kinematic
cl_efcal0_rawtopo;	cl_efcal0_caltopo;	vector<float>	energy in electromagnetic forward calorimeter	
cl_efcal1_rawtopo;	cl_efcal1_caltopo;	vector<float>	energy in hadronic forward calorimeter sampling 1	Cluster Kinematic
cl_efcal2_rawtopo;	cl_efcal2_caltopo;	vector<float>	energy in hadronic forward calorimeter sampling 2	
cl_ehcal0_rawtopo;	cl_ehcal0_caltopo;	vector<float>	energy in hadronic endcap sampling 0	Cluster Kinematic
cl_ehcal1_rawtopo;	cl_ehcal1_caltopo;	vector<float>	energy in hadronic endcap sampling 1	
cl_ehcal2_rawtopo;	cl_ehcal2_caltopo;	vector<float>	energy in hadronic endcap sampling 2	Cluster Kinematic
cl_ehcal3_rawtopo;	cl_ehcal3_caltopo;	vector<float>	energy in hadronic endcap sampling 3	
cl_eta0_rawtopo;	cl_eta0_caltopo;	vector<float>	pseudo-rapidity in barrel pre-sampler	Cluster Kinematic
cl_eta1_rawtopo;	cl_eta1_caltopo;	vector<float>	pseudo-rapidity in barrel sampling 1	
cl_eta2_rawtopo;	cl_eta2_caltopo;	vector<float>	pseudo-rapidity in barrel sampling 2	Cluster Kinematic
cl_eta3_rawtopo;	cl_eta3_caltopo;	vector<float>	pseudo-rapidity in barrel sampling 3	
cl_nemb0_rawtopo;	cl_nemb0_caltopo;	vector<long>	# cells in barrel pre-sampler	Cluster Kinematic
cl_nemb1_rawtopo;	cl_nemb1_caltopo;	vector<long>	# cells in barrel sampling 1	
cl_nemb2_rawtopo;	cl_nemb2_caltopo;	vector<long>	# cells in barrel sampling 2	Cluster Kinematic
cl_nemb3_rawtopo;	cl_nemb3_caltopo;	vector<long>	# cells in barrel sampling 3	
cl_neme0_rawtopo;	cl_neme0_caltopo;	vector<long>	# cells in endcap pre-sampler	Cluster Kinematic
cl_neme1_rawtopo;	cl_neme1_caltopo;	vector<long>	# cells in endcap sampling 1	
cl_neme2_rawtopo;	cl_neme2_caltopo;	vector<long>	# cells in endcap sampling 2	Cluster Kinematic
cl_neme3_rawtopo;	cl_neme3_caltopo;	vector<long>	# cells in endcap sampling 3	
cl_nfcad0_rawtopo;	cl_nfcad0_caltopo;	vector<long>	# cells in electromagnetic forward calorimeter	Cluster Kinematic
cl_nfcad1_rawtopo;	cl_nfcad1_caltopo;	vector<long>	# cells in hadronic forward calorimeter sampling 1	
cl_nfcad2_rawtopo;	cl_nfcad2_caltopo;	vector<long>	# cells in hadronic forward calorimeter sampling 2	Cluster Kinematic
cl_nheco_rawtopo;	cl_nheco_caltopo;	vector<long>	# cells in hadronic endcap sampling 0	
cl_nhec1_rawtopo;	cl_nhec1_caltopo;	vector<long>	# cells in hadronic endcap sampling 1	Cluster Kinematic
cl_nhec2_rawtopo;	cl_nhec2_caltopo;	vector<long>	# cells in hadronic endcap sampling 2	
cl_nhec3_rawtopo;	cl_nhec3_caltopo;	vector<long>	# cells in hadronic endcap sampling 3	Cluster Kinematic
cl_phi2_rawtopo;	cl_phi2_caltopo;	vector<float>	azimuth in barrel sampling 2	



Slide 43

More
details
for
Clusters

Uncalibrated TopoClusters	Calibrated TopoClusters	Type	Comment	
ci_etlib0_rawtopo;	ci_etlib0_caltopo;	vector<float>*	energy in tile barrel sampling 0	Cluster Variables in Tile Calorimeter
ci_etlib1_rawtopo;	ci_etlib1_caltopo;	vector<float>*	energy in tile barrel sampling 1	
ci_etlib2_rawtopo;	ci_etlib2_caltopo;	vector<float>*	energy in tile barrel sampling 2	
ci_etlib00_rawtopo;	ci_etlib00_caltopo;	vector<float>*	energy in extended tile sampling 0	
ci_etlib01_rawtopo;	ci_etlib01_caltopo;	vector<float>*	energy in extended tile sampling 1	
ci_etlib02_rawtopo;	ci_etlib02_caltopo;	vector<float>*	energy in extended tile sampling 2	
ci_etlib03_rawtopo;	ci_etlib03_caltopo;	vector<float>*	energy in the sampling 3	
ci_etlib10_rawtopo;	ci_etlib10_caltopo;	vector<float>*	energy in tile sampling 1	
ci_etlib11_rawtopo;	ci_etlib11_caltopo;	vector<float>*	energy in tile sampling 2	
ci_etlib12_rawtopo;	ci_etlib12_caltopo;	vector<float>*	energy in the sampling 3	
ci_nlib00_rawtopo;	ci_nlib00_caltopo;	vector<long>*	# cells in tile barrel sampling 0	
ci_nlib01_rawtopo;	ci_nlib01_caltopo;	vector<long>*	# cells in tile barrel sampling 1	
ci_nlib02_rawtopo;	ci_nlib02_caltopo;	vector<long>*	# cells in the barrel sampling 2	
ci_nlib000_rawtopo;	ci_nlib000_caltopo;	vector<long>*	# cells in extended tile sampling 0	
ci_nlib001_rawtopo;	ci_nlib001_caltopo;	vector<long>*	# cells in extended tile sampling 1	
ci_nlib002_rawtopo;	ci_nlib002_caltopo;	vector<long>*	# cells in extended tile sampling 2	
ci_nlib003_rawtopo;	ci_nlib003_caltopo;	vector<long>*	# cells in the gap sampling 3	
ci_nlib010_rawtopo;	ci_nlib010_caltopo;	vector<long>*	# cells in tile gap sampling 1	
ci_nlib011_rawtopo;	ci_nlib011_caltopo;	vector<long>*	# cells in the gap sampling 2	
ci_nlib012_rawtopo;	ci_nlib012_caltopo;	vector<long>*	# cells in tile gap sampling 3	
ci_center_lambda_rawtopo;	ci_center_lambda_caltopo;	vector<float>*	central cluster depth in calorimeter	Cluster Moments (Shapes)
ci_center_x_rawtopo;	ci_center_x_caltopo;	vector<float>*	barycenter x	
ci_center_y_rawtopo;	ci_center_y_caltopo;	vector<float>*	barycenter y	
ci_center_z_rawtopo;	ci_center_z_caltopo;	vector<float>*	barycenter z	
ci_delta_alpha_rawtopo;	ci_delta_alpha_caltopo;	vector<float>*	angular distance principal axis-vertex direction	
ci_delta_phi_rawtopo;	ci_delta_phi_caltopo;	vector<float>*	azimuthal distance principal axis-vertex direction	
ci_delta_theta_rawtopo;	ci_delta_theta_caltopo;	vector<float>*	polar distance principal axis-vertex direction	
ci_eng_frac_core_rawtopo;	ci_eng_frac_core_caltopo;	vector<float>*	energy fraction of cluster core	
ci_eng_frac_em_rawtopo;	ci_eng_frac_em_caltopo;	vector<float>*	energy fraction in electromagnetic calorimeter	
ci_eng_frac_max_rawtopo;	ci_eng_frac_max_caltopo;	vector<float>*	energy fraction of cell with maximum signal	
ci_lateral_rawtopo;	ci_lateral_caltopo;	vector<float>*	normalized lateral spread	
ci_longitudinal_rawtopo;	ci_longitudinal_caltopo;	vector<float>*	normalized longitudinal spread	
ci_m1_dens_rawtopo;	ci_m1_dens_caltopo;	vector<float>*	first moment energy density	
ci_m1_eta_rawtopo;	ci_m1_eta_caltopo;	vector<float>*	pseudorapidity first moment	
ci_m1_phi_rawtopo;	ci_m1_phi_caltopo;	vector<float>*	azimuth first moment	
ci_m2_dens_rawtopo;	ci_m2_dens_caltopo;	vector<float>*	second moment energy density	
ci_m2_lambda_rawtopo;	ci_m2_lambda_caltopo;	vector<float>*	second longitudinal moment	
ci_m2_r_rawtopo;	ci_m2_r_caltopo;	vector<float>*	second radial moment	



Slide 44

Conclusions

- In general we expect the jet and missing E_T performance at the LHC to meet most physics requirements, with some challenges remaining for the jet energy scale error;
- Further improvements are depending on a significant increase of the prediction power of hadronic shower models in Geant4 - continuing focus on validation using testbeam data;
- A new hadronic calibration model in ATLAS using local cluster calibration for jets and missing E_T looks very promising and is available for full evaluation;
- We still miss systematic evaluations of jet shapes and topologies in the presence of pile-up;